Proceedings of the Twenty-first (2011) International Offshore and Polar Engineering Conference
Maui, Hawaii, USA, June 19-24, 2011

ISBN 978-1-880653-96-8 (Set); ISSN 1098-6189 (Set); www.isope.org

Development of 3D Morphodynamic Model Considering Wave-current Interaction

Ahmed Khaled Seif, Masamitsu Kuroiwa, and Yuhei Matsubara
Department of Civil Engineering, Tottori University, Tottori, Japan

Mazen Abualtayef
Department of Environmental Engineering, The Islamic University of Gaza, Palestine

Hajime Mase
Disaster Prevention Research Institute, Kyoto University, Kyoto, Japan

ABSTRACT

This study develops a three dimensional morphodynamic model around coastal structures considering a wave-current interaction. In the wave model, the current effects on wave breaking and energy dissipation are taken into account as well as the wave diffraction effect. Furthermore, the nearshore current model was modified in association with the surface roller effect. Firstly, an experimental data set from the Large Scale Sediment Transport Facility was used to evaluate the predictive capability of the model. Secondly, several model tests against detached breakwaters were carried out to investigate the performance of the model. Finally, the model was applied to Kunnui fishing port for the prediction of the bathymetry after 1 year, and for the calibration and verification of the morphodynamics around the coastal structures. For the model tests, the performance of the model was investigated; and for Kunnui fishing port, the model result shows a good agreement with the field observation. It was found that the wave-current interaction with the surface roller was significantly playing an important role in the prediction of the three dimensional morphodynamics computation.

KEY WORDS: 3D morphodynamic model; Quasi-3D; wave-current interaction; coastal structures; detached breakwater; Kunnui port.

INTRODUCTION

An accurate prediction of waves and nearshore currents is a key role in solving coastal engineering problems, especially of those related to beach morphological evolution. Previously, some three dimensional (3D) morphodynamic models using a quasi three dimensional (Q-3D) model around coastal structures have been proposed (e.g. De Vried *et al*., 1988; and Bos *et al*., 1996). However, the model prediction was not accurate, and the major reason is due to that the nearshore waves and current fields were independently determined without considering the wave-current interaction. Therefore, in order to predict the morphodynamics around the coastal structures with better accuracy, a 3D morphodynamic model that considering the wave-current interaction is needed. Recently, the authors have proposed a new Q-3D model with considering the wave-current interaction and the surface roller (Khaled Seif *et al*., 2010). The main goal of this study is to develop a 3D numerical model to predict the morphodynamic around coastal structures with considering the wave-current interaction.

NUMERICAL MODEL

The present model consists of four modules, which are: wave module, nearshore current module, sediment transport module, and water depth change module. The wave and nearshore current fields are dependently determined with the consideration of the wave-current interaction.

Wave Module

The wave module is based on the multi-directional random wave model, which is based on the wave action balance equation associated with energy dissipation terms for the wave breaking and wave diffraction (Mase *et al*., 2004). In this module, the wave-current interaction was calculated. The governing wave action balance equation with the wave diffraction effects is

$$\frac{\partial\left(C_x N\right)}{\partial x}+\frac{\partial\left(C_y N\right)}{\partial y}+\frac{\partial\left(C_\theta N\right)}{\partial \theta}= \frac{\kappa}{2\sigma}\left\{\left(CC_g\cos^2\theta N_y\right)_y-\frac{1}{2}CC_g\cos^2\theta N_{yy}\right\}-\varepsilon_b N \quad (1)$$

where N is the wave action density, defined as the wave energy density divided by the angular frequency σ relative to the current (Doppler shift). The horizontal coordinates are x and y, and θ is the wave direction measured counterclockwise from the x-axis. As suggested by Mase (2001), the default value of k =2.5 was used for the diffraction intensity parameter. C and C_g are the wave celerity and group velocity, respectively. The characteristic wave velocities with respect to x, y, and θ coordinates are accordingly C_x, C_y and C_θ as defined by

$$C_x = C_g\cos\theta+\tilde{U} \quad (2)$$

$$C_y = C_g \sin\theta + \tilde{V} \tag{3}$$

$$C_\theta = \frac{\sigma}{\sinh 2kh}\left(\sin\theta\frac{\partial h}{\partial x} - \cos\theta\frac{\partial h}{\partial y}\right) + \cos\theta\sin\theta\frac{\partial \tilde{U}}{\partial x} - \cos^2\frac{\partial \tilde{U}}{\partial y} + sin^2\theta\frac{\partial \tilde{V}}{\partial x} - \sin\theta\cos\theta\frac{\partial \tilde{V}}{\partial y} \tag{4}$$

where $\tilde{U}$ and $\tilde{V}$ are the depth-averaged steady currents in the *x* and *y* direction, and *k* is the wave number. The relationships between the relative angular frequency σ, the absolute angular frequency ω, the wave number vector **k**, the current velocity vector $\tilde{U}$, and the water depth h are shown in the following equations

$$\sigma^2 = g|\mathbf{k}|\tanh|\mathbf{k}|h \tag{5}$$

$$\sigma = \omega - \mathbf{k}\bullet\tilde{\mathbf{U}} \tag{6}$$

In Eq. (1), the parameterized function ε_b describes the mean energy dissipation rate per unit horizontal area due to the wave breaking. The importance of this function was examined for four wave breaking formula by Zheng *et al*. (2008). In this study, the parameterized wave breaking function for wave energy dissipation was calculated from the following expression for bulk energy dissipation with the ambient current, which proposed by Chawla and Kirby (2002):

$$\langle D\rangle = \frac{3\lambda\rho}{32\sqrt{\pi}}\sqrt{\frac{(g\bar{k})^3}{\tanh\bar{k}h}}\left(\frac{\bar{k}}{\gamma\tanh\bar{k}h}\right)^2 \times H_{rms}^5\left[1-\left\{1+\left(\frac{\bar{k}H_{rms}}{\gamma\tanh\bar{k}h}\right)^2\right\}^{-5/2}\right] \tag{7}$$

where $\langle D\rangle$ is the bulk energy dissipation by all breaking waves, H_{rms} is the root-mean-square wave height, and $\bar{k}$ is the wave number corresponding to the mean angular frequency $\bar{\sigma}$, and the scaling parameters λ and γ are set to 0.4 and 0.6, respectively.

The wave breaking energy dissipation coefficient ε_b is calculated as

$$\varepsilon_b = \langle D\rangle \Big/ \left(0.125\rho g H_{rms}^2\right)\bar{\sigma} \tag{8}$$

Furthermore, the energy balance equation was used in association with the surface roller term, which is based on the equation of Dally and Brown (2002) as follows

$$-D_b + \frac{\partial}{\partial x}\left(\frac{1}{2}MC_r^2\cos^2\bar{\theta}\right) + \frac{\partial}{\partial y}\left(\frac{1}{2}MC_r^2\sin^2\bar{\theta}\right) = -g\beta_D M \tag{9}$$

where D_b is the wave breaking energy dissipation, M is the wave-period-averaged mass flux, C_r is the roller speed ($\approx C$), and the roller dissipation coefficient β_D was set to 0.1 The stresses due to the rollers are determined as follows

$$R_{xx} = MC_r\cos^2\bar{\theta} \tag{10}$$

$$R_{yy} = MC_r\sin^2\bar{\theta} \tag{11}$$

$$R_{xy} = R_{yx} = MC_r\sin 2\bar{\theta} \tag{12}$$

Nearshore current Module

The nearshore current module is based on the Q-3D nearshore current model proposed by Kuroiwa *et al*. (2002). The governing equations are defined as follows

$$\frac{\partial U}{\partial t} + U\frac{\partial U}{\partial x} + V\frac{\partial U}{\partial y} + W\frac{\partial U}{\partial z} = -g\frac{\partial \bar{\zeta}}{\partial x} - \frac{\partial(S_{xx}+R_{xx})}{\partial x} - \frac{\partial(S_{xy}+R_{xy})}{\partial y} + \frac{\partial}{\partial x}\left(v_h\frac{\partial U}{\partial x}\right) + \frac{\partial}{\partial y}\left(v_h\frac{\partial U}{\partial y}\right) + \frac{\partial}{\partial z}\left(v_v\frac{\partial U}{\partial z}\right) \tag{13}$$

$$\frac{\partial V}{\partial t} + U\frac{\partial V}{\partial x} + V\frac{\partial V}{\partial y} + W\frac{\partial V}{\partial z} = -g\frac{\partial \bar{\zeta}}{\partial y} - \frac{\partial(S_{yx}+R_{yx})}{\partial x} - \frac{\partial(S_{yy}+R_{yy})}{\partial y} + \frac{\partial}{\partial x}\left(v_h\frac{\partial V}{\partial x}\right) + \frac{\partial}{\partial y}\left(v_h\frac{\partial V}{\partial y}\right) + \frac{\partial}{\partial z}\left(v_v\frac{\partial V}{\partial z}\right) \tag{14}$$

where *U*, *V* and *W* are the steady current velocities in the *x*, *y* and *z* directions. S_{xx}, S_{yy}, S_{xy}, and S_{yx} represent the terms of excess momentum fluxes due to the waves. v_v and v_h represents the turbulent eddy viscosity coefficient in the vertical and horizontal direction, respectively. v_v is estimated by Tsuchiya *et al*. (1986):

$$\nu_v = A_v C\, H_{rms} \tag{15}$$

where A_v is a dimensionless coefficient set at 0.01.

and v_h is estimated by Larson *et al*. (2002):

$$\nu_h = \Lambda\, \hat{u}_w H_{rms} \tag{16}$$

where Λ is a constant value set at 1.50, $\hat{u}_w$ is the maximum water particle velocity in the *x* direction.

The radiation stress part was modified by adding the momentum fluxes term due to the surface roller as R_{xx}, R_{yy}, R_{xy}, and R_{yx}. The continuity equation is expressed as

$$\frac{\partial U}{\partial x} + \frac{\partial V}{\partial y} + \frac{\partial W}{\partial z} = 0 \tag{17}$$

The depth-integrated continuity equation is

$$\frac{\partial \bar{\zeta}}{\partial t} + \frac{\partial \tilde{U}(h+\bar{\zeta})}{\partial x} + \frac{\partial \tilde{V}(h+\bar{\zeta})}{\partial y} = 0 \tag{18}$$

where $\tilde{U}$ and $\tilde{V}$ are the depth-averaged steady currents, and $\bar{\zeta}$ is the mean water level.

An iterative feed back process between the wave module and the nearshore current module was carried out to obtain the steady state condition, as shown in Fig.1. In order to reach the steady state condition, the wave field calculation was updated by taking the average wave field between the previous and present iteration to compute the nearshore current field for the next iteration.

Sediment Transport Rate Module

According to Kuroiwa *et al*. (2000), the total sediment transport rates in the cross-shore and alongshore direction are given by

$$q_x = q_{wx} + q_{cx} + q_{sx} \tag{19}$$

$$q_y = q_{wy} + q_{cy} + q_{sy} \tag{20}$$

where q_{wx} and q_{wy} are the bed loads due to wave particle velocities at bottom. q_{cx} and q_{cy} are the bed loads due to steady current at bottom. The sediment transport rates are determined by using the method proposed by Watanabe *et al*. (1986), which are given by:

$$q_{wx} = A_w\left(u_*^2 - u_{*c}^2\right)\hat{u}_w / g\,,\ \ q_{wy} = A_w\left(u_*^2 - u_{*c}^2\right)\hat{v}_w / g \tag{21}$$

$$q_{cx} = A_c\left(u_*^2 - u_{*c}^2\right)U_b / g\,,\ \ q_{cy} = A_c\left(u_*^2 - u_{*c}^2\right)V_b / g \tag{22}$$

where A_w and A_c are dimensionless coefficients. These coefficients are given by a function of median diameter d_{50} (Shimizu *et al*., 1996b). u_* is the friction velocity. u_{*c} is the critical friction velocity. The friction velocity u_* presented by Sawaragi *et al.* (1985) was adapted in order to take account of the interaction of waves and steady currents. $\hat{u}_w$ and $\hat{v}_w$ are the maximum water particle velocities at sea bottom based on the liner wave theory. U_b and V_b are steady current velocities at sea bottom. The suspended sediment transport rates q_{sx} and q_{sy} are determined by multiplying local vertical profiles of current velocities and sediment concentrations, and then integrating from the bottom to the mean water surface. The sediment transport rates in the cross-shore (x) and alongshore (y) directions are expressed as

$$q_{sx} = \int_{-h}^{\bar{\zeta}} c(z)U(x,y,z)dz\,,\ q_{sy} = \int_{-h}^{\bar{\zeta}} c(z)V(x,y,z)dz \tag{23}$$

U and V are the steady current velocities, which are determined from the Q-3D model. The concentration $c(z)$ can be expressed as

$$c(z) = c_b\ exp\left(-\frac{w_f}{\varepsilon_s}z\right) \tag{24}$$

c_b is the concentration at which the sediment starts moving. w_f is the fall velocity of sand. ε_s is the diffusion coefficient of sand. The c_b is given by Shibayama and Rattanapitikon *et al.* (1993) as

$$c_b = c_s\frac{10}{3}\frac{(\phi - 0.05)\nu}{b\sqrt{sgd_{50}}} \tag{25}$$

C_s is the dimensionless coefficient. d is the mean diameter of sand particle. b is the boundary thickness defined by $b=100\ d_{50}$. s is the specific gravity in the water.

Water Depth Change Module

The changes in bottom elevation were calculated using the continuity equation of sediment transport rate proposed by Watanabe *et al*. (1986), which is expressed as

$$\frac{\partial h}{\partial t} = \frac{1}{1-\lambda_c}\left\{\frac{\partial}{\partial x}\left(q_x + \varepsilon_s|q_x|\frac{\partial h}{\partial x}\right) + \frac{\partial}{\partial y}\left(q_y + \varepsilon_s|q_y|\frac{\partial h}{\partial y}\right)\right\} \tag{26}$$

where E_s is the constant value. λ_c is the porosity of the bed. The profile changes in the run-up region are also determined from the continuity equation and the shoreline is treated as a moving boundary. In order to predict the final bathymetry, the new bottom topography was feedback into the hydrodynamic and sediment transport computations, as shown in Fig.1

MODEL TESTS

LSTF Experimental Model Test

Firstly, the present model was applied to the longshore current experimetal model under an irrigular wave from the Large Scale Sediment Transport Facility (LSTF), performed by Hamilton and Ebersole (2001), to validate the hydrodynamic model.

LSTF model setup

The computation was performed in a concrete beach with alongeshore dimension of 31m and a cross-shore dimension of 21m, and the plane slope was 1:30. The grid size was Δx=Δy=0.5m. The significant wave height at the offshore boundary was 0.225m, the significant wave period was 2.5s, and the wave direction at the wave generations was 10 degree. In Eq.7, λ was set to 1.8 in order to calibrate the nearshore current field.

LSTF model results

The computed results of our model were compared against the experiemntal model results. Figs.2(a) and (b) show comparisons between the computed and measured wave height distribution, and longeshore current, with and without the wave-current interaction and the surface roller effect. The model was run until the steady state with the consideration of wave-current interaction was reached. The prediction of significant wave height was in a good agreement when the wave-current interaction was considered, as shown in Fig.2(a). The computed results of longshore currents with the effect of the surface roller was not only shifted the peak toward the shoreline, but also increased the maximum current magnitudes in the surf zone, as shown in Fig.2(b). From these results, it was found that the computed wave height distribution and longeshore current were in a good agreement with the experiemental results.

Numerical Model Tests

Several model tests associated with detached breakwaters with and without the wave-current interaction were carried out to investigate the performance of the model, and the planform development behind a single detached breakwater.

Numerical model setup

The computations were performed on an area of 0.6km alongshore and 0.6km cross-shore. The initial bathymetry with a gradient of 1:50 was set. The grid size was 10m (Δx=Δy). The significant wave height at the offshore boundary was 1.5m, and the significant wave period was 7.0s. According to Johnson *et al*. (1994), the equilibrium planform that develops behind a single detached breakwater is mainly governed by its length and the distance to the initial shoreline. Therefore, the length W_B of the breakwater and its distance to the initial shoreline X_B are systematically varied in the tests. The computation conditions are summarized in Table 1.

Numerical model results

Fig.3 and Fig.4 show the computed results of a) wave height distribution, b) bottom current velocity, c) surface current velocity, and d) final bathymetry around the detached breakwater for Test 1, without and with the wave-current interaction, respectively. From these figures, it was found that by considering the wave-current interaction, the wave height distribution behind the detached breakwater, and the magnitude of the current velocities were changed. Figs. 3(d), 4(d) show the computed final bathymetry for Test 3 without and with the wave-current interaction, respectively. From these figures, it was found that the bathymetry behind the breakwater with the interaction was deeper than without the interaction. Furthermore, the shoreline was qualitatively produced when the wave-current interaction considered. This is due to the model run reached the steady state condition only when the wave-current interaction was considered. Comparisons between the computed results of Test 3, without and with the wave-current interaction were conducting. From these comparisons, it was found that the wave height distribution and the magnitude of the current velocities behind the detached breakwater when considering the wave-current interaction were different from those without considering the

wave-current interaction, as shown in Fig.5 and Fig.6. Figs. 5(d), 6(d) show the computed final bathymetry for Test 3 without and with the wave-current interaction, respectively. From these figures, it was found that a double-salient was produced with considering the wave-current interaction, while a single-salient was produced without considering the wave-current interaction. Similar comparisons were conducted on the rest of model tests (Test 2, and Test 4), and the obtained results gave an assurance to the results above.

In order to investigate the planform development behind a single detached breakwater, comparisons between the computed bathymetries of the model tests were done. From these comparisons it was found that a deposition occurs behind the detached breakwater whereas the current decreases and erosion occurs on both side of it due to the accelerated current towards the lee of the breakwater. These results are the same as frequently observed in the field.

As shown in the figures (Fig.3 to Fig.8) the type of the planform development behind a single detached breakwater depends on the dimensions of the breakwater (W_B and X_B), in addition whether the wave-current interaction was considered or not. It was concluded that by increasing the length of the detached breakwater, the bathymetry behind it was shallower. Also, by decreasing the breakwater distance to the shoreline, the bathymetry is affected behind the breakwater, especially the shoreline.

As a conclusion of the model tests, it was found that the wave-current interaction with the surface roller was significantly playing an important role in the prediction of the morphodynamic computation around the coastal structures.

Table 1 Computation conditions of model tests

Model test	Parameters		
	Breakwater length, W_B, m	Distance from shoreline, X_B, m	W_B / X_B
Test(1)	210	300	0.7
Test(2)	210	210	1.0
Test(3)	210	150	1.4
Test(4)	330	150	2.2

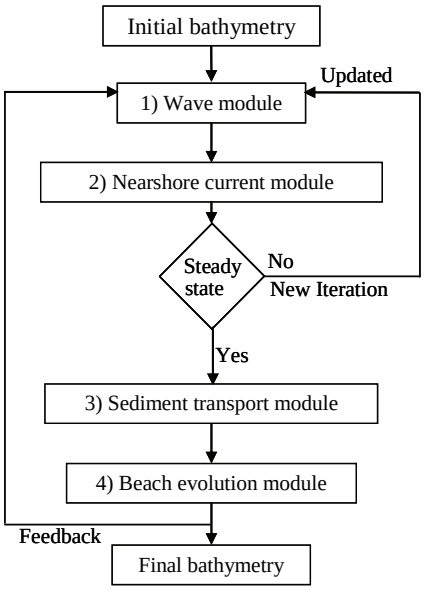

Fig.1 Flowchart of the numerical model.

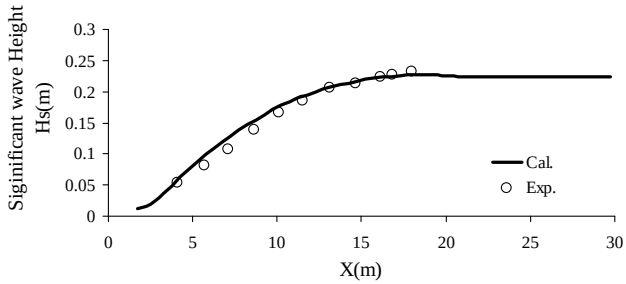

Fig.2(a) Computed and observed wave height distribution.

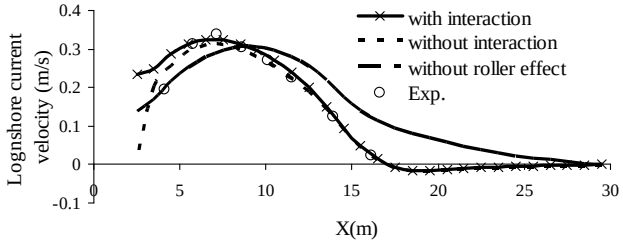

Fig.2(b) Computed and observed longshore current velocities.

MODEL VERIFICATION

The presented model was further verified and applied for one year tombolo formation behind Kunnui fishing port at Hokkaido, Japan (Kawaguchi *et al*., 1994). The Kunnui fishing port was planned in 1985 and the construction was completed in 1994. Before the construction completion of the port, the bottom contours were almost parallel, and after one year, a tombolo was rapidly formed behind the port in the period between 1989 and 1990, as shown in Fig.9 and Fig.10. In this study, the beach evolutions from 1989 to 1990 were simulated to verify the present model.

Model Setup

The computation was performed in an area of 1.0km in the alongshore direction and 0.8km in the cross-shore direction. The initial bathymetry with the gradient of 1:90 was set. The grid size was 10m. In order to predict the beach evolution, the significant wave height of less than 1m was omitted because the waves can not contribute against the beach evolution (Shimizu *et al*., 1996a). Therefore, the duration of which the beach evolution was generated in 1 year was 8 days. The time variation of wave data input at the offshore boundary was taken into account. The computations of the wave and current modules were repeated 6 times to reach 1 year beach evolution, as shown in Table 2. The principal wave direction was perpendicular to the shoreline. The median diameter of sand particle was 0.20mm.

Table 2 Computational conditions of the model.

Wave Condition	Period, day	H_s	T_s
1,3,4,6	2.0	1.25	8.0
2,5	0.2	2.0	10.0

Results and Discussion

Fig.11 illustrates the computed bathymetry after 1 year (1989-1990) without considering the wave-current interaction. Fig.12 illustrates the computed bathymetry after 1 year (1989-1990) with considering the wave-current interaction. Comparing with the measured bathymetry in 1990, it was found that the tombolo was formed behind the Kunnui

fishing port. Although the depth contour lines of 1m, 2m and 3m were advanced to the offshore direction due to the circulation behind the fishing port, the computed shoreline change with considering the wave-current interaction is slightly different than the field measurement. The shoreline and bottom topography changes such as the formation of tombolo behind the port could be qualitatively computed.

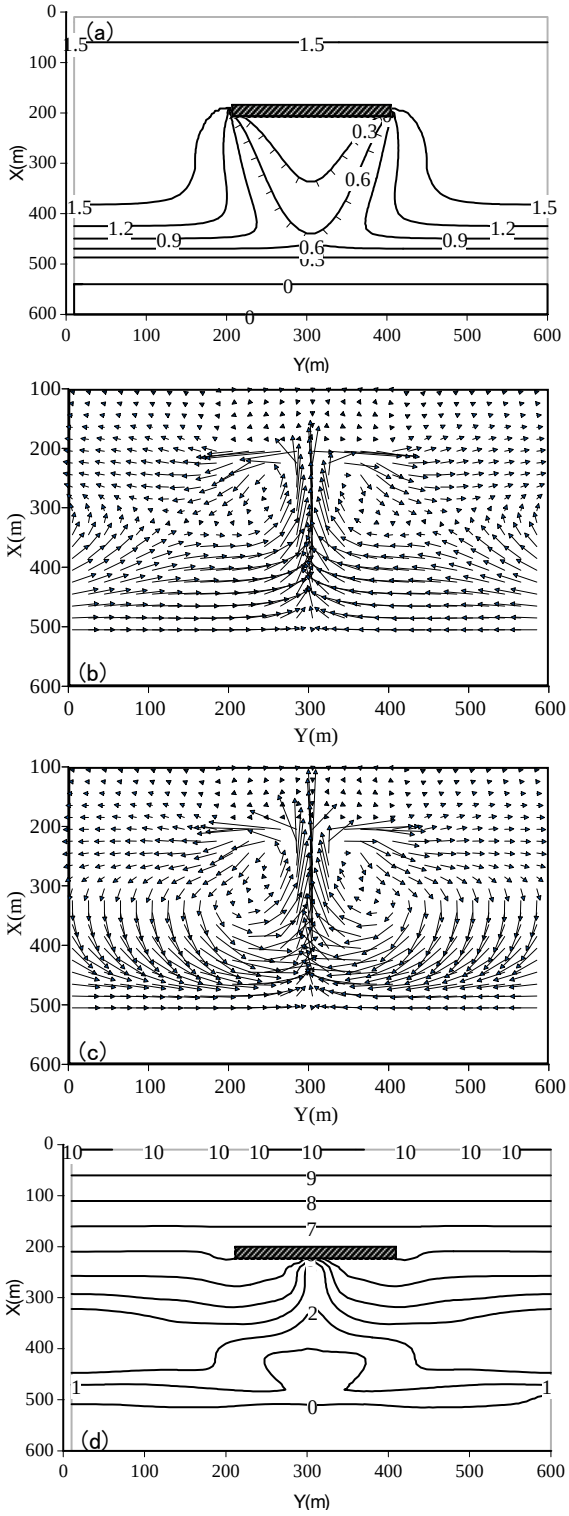

Fig.3 Computed results for Test 1 without considering the wave-current interaction. (a) significant wave height distribution, (b) bottom current velocity, (c) surface current velocity, and (d) final bathymetry.

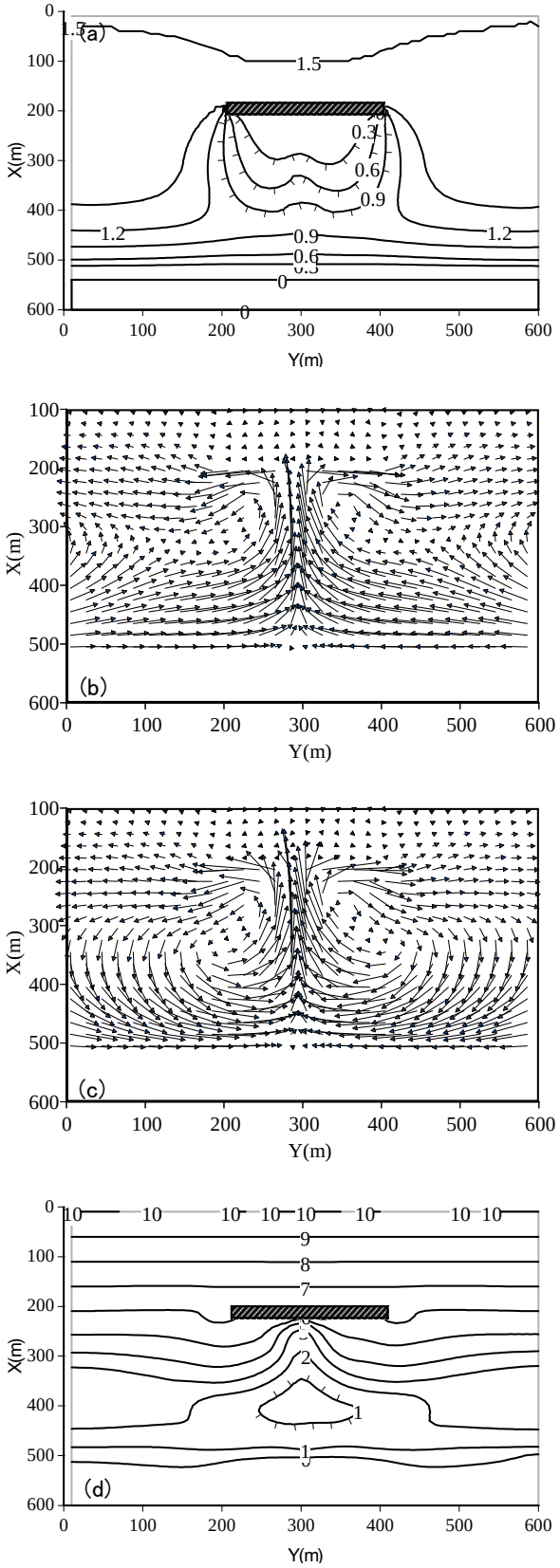

Fig.4 Computed results for Test 1 with considering the wave-current interaction. (a) significant wave height distribution, (b) bottom current velocity, (c) surface current velocity, and (d) final bathymetry.

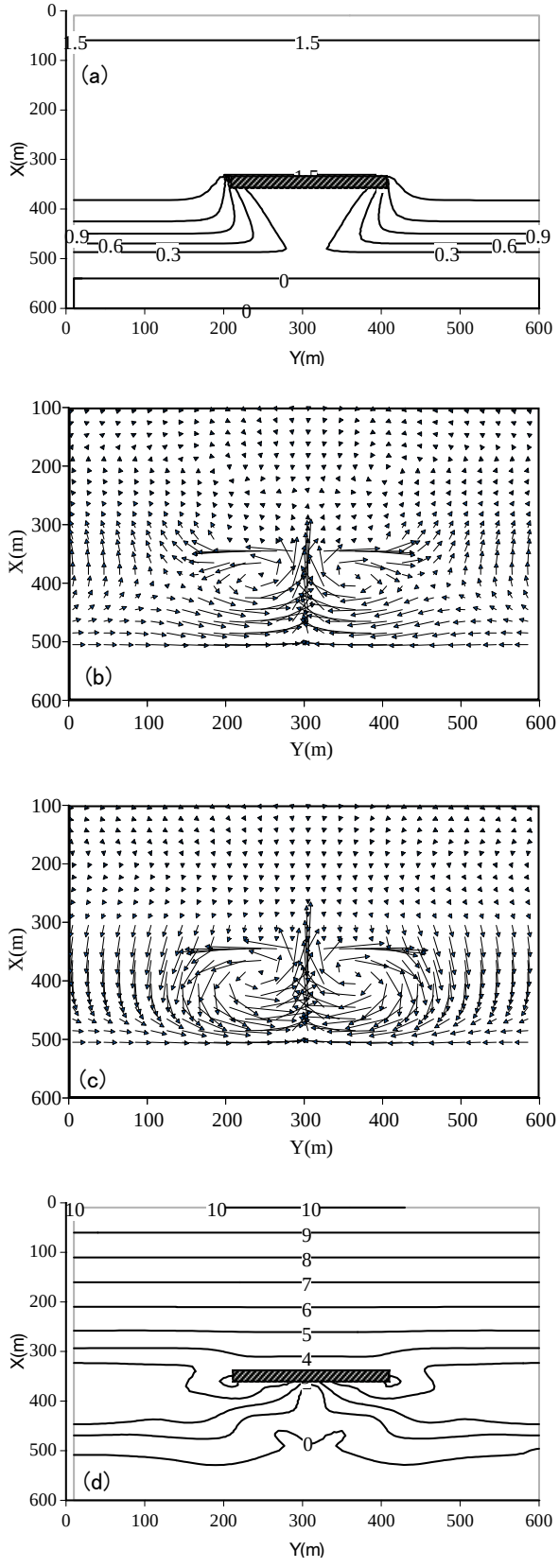

Fig.5 Computed results for Test 3 without considering the wave-current interaction. (a) significant wave height distribution, (b) bottom current velocity, (c) surface current velocity, and (d) final bathymetry.

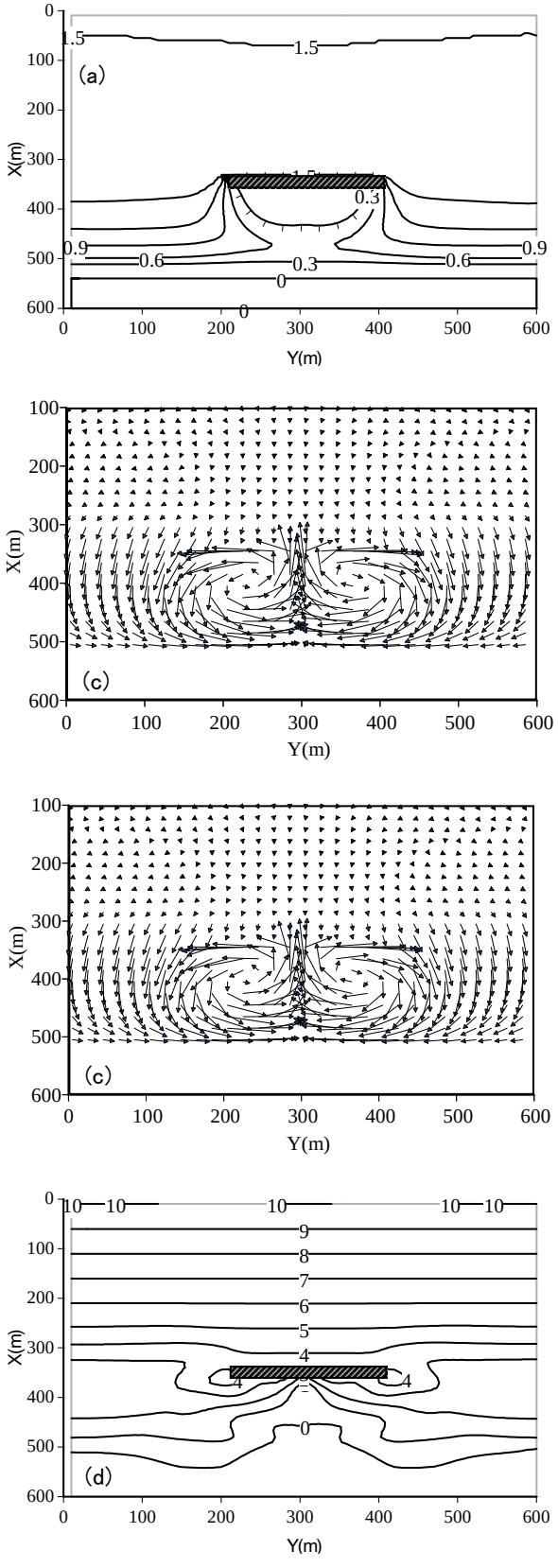

Fig.6 Computed results for Test 3 with considering the wave-current interaction. (a) significant wave height distribution, (b) bottom current velocity, (c) surface current velocity, and (d) final bathymetry.

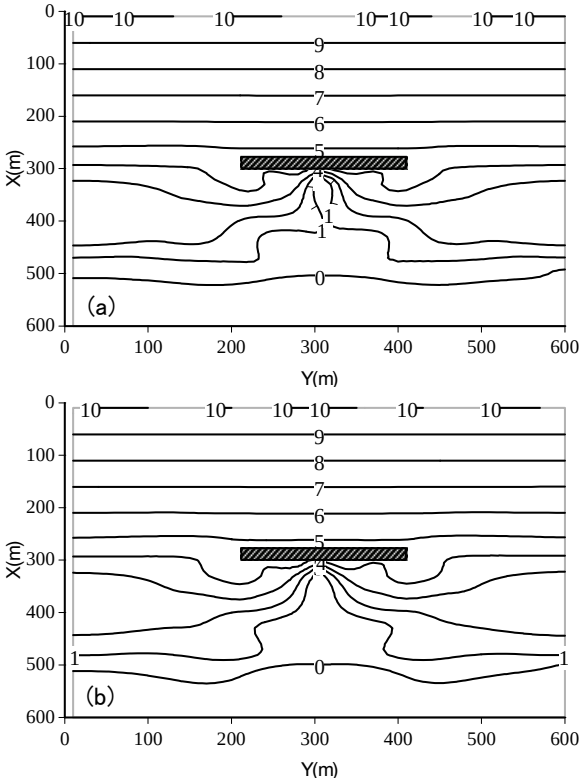

Fig.7 Computed final bathymetry (a) without and (b) with interaction for Test 2.

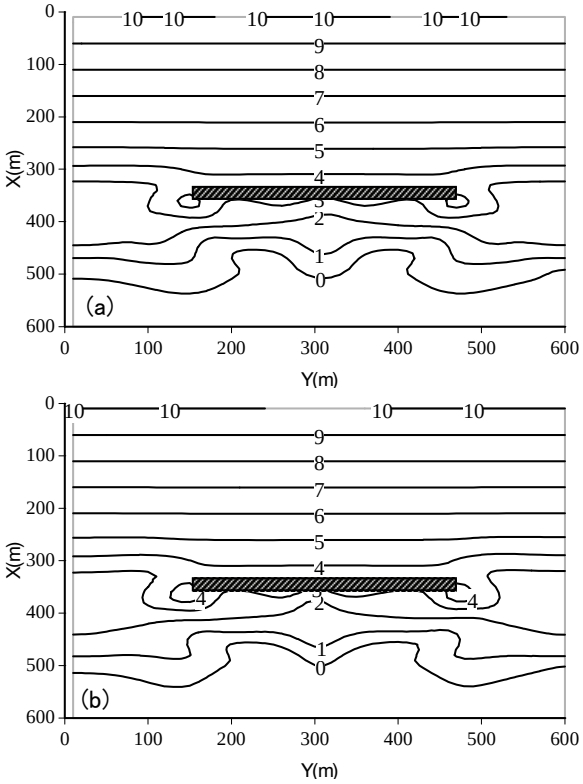

Fig.8 Computed final bathymetry (a) without and (b) with interaction for Test 4.

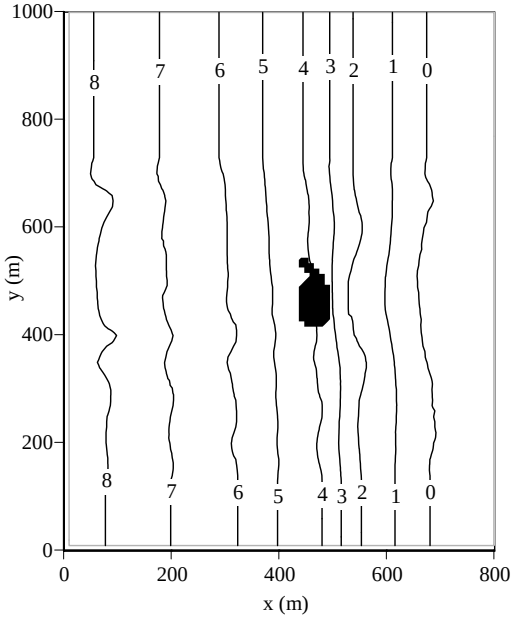

Fig.9 Observed bathymetry in 1989.

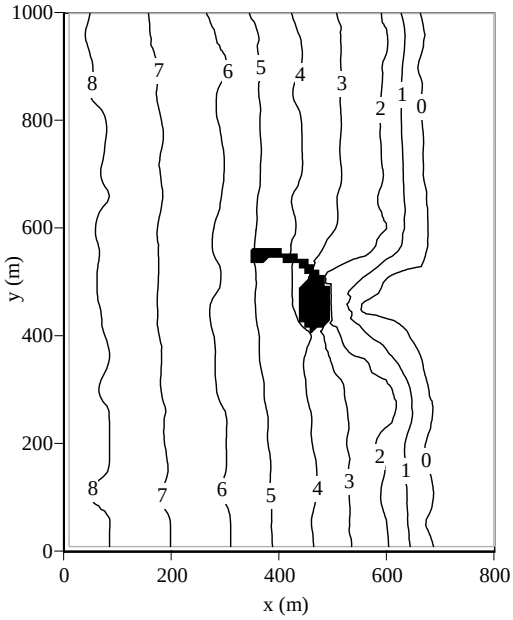

Fig.10 Observed bathymetry in 1990.

CONCLUSIONS

In this study, the morphodynamic model around coastal structures was developed. The applicability of the model was demonstrated through several numerical tests and compared against experimental and field observations. The new proposed morphodynamic model shows good agreement with the observations. Furthermore, it was found that the wave-current interaction with the surface roller was significantly playing an important role for the prediction of the 3D morphodynamics computation. The computed results of the rest of model tests will be presented in the conference.

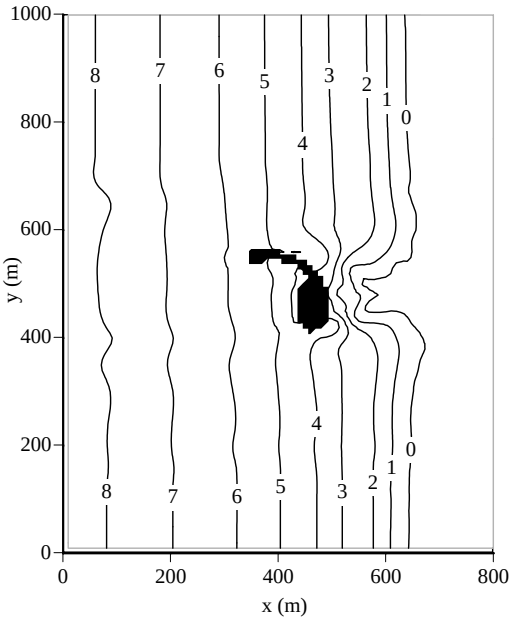

Fig.11 Computed bathymetry without interaction.

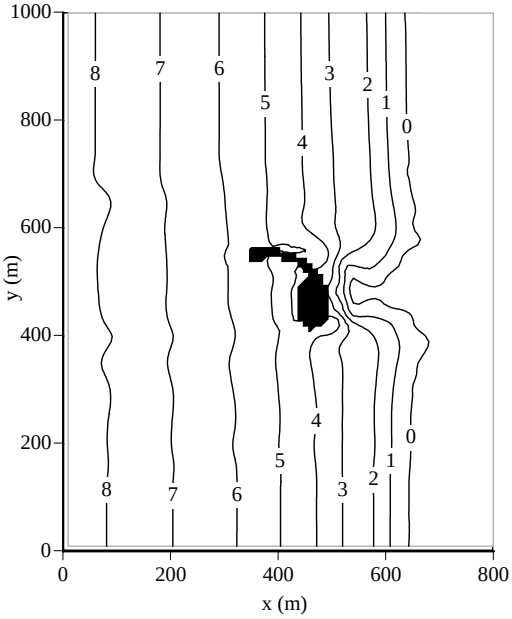

Fig.12 Computed bathymetry with interaction.

REFERENCES

Bos, J.K., Roelvink, J.A. and Dingemans, M.W (1996). Modeling the impact of detached breakwaters on the coast. *Proceedings of the 25th International Conference on Coastal Engineering*, pp.2022-2035.

Chawla, A., and Kirby, J.T. (2002). Monochromatic and random wave breaking at blocking points. *Journal of Geophysical Research*, 107, No. C7.

Dally, W.R. and Brown, Ch.A. (2002). A modeling investigation of the breaking wave roller with application to cross-shore currents. *Journal of Geophysical Research*, 100, No. C12, pp.873-883.

De Vriend, H.J. and Ribberink, J.S. (1988). *A quasi-3D mathematical model of coastal morphology*. *Proc. of the 21th ICCE*, pp.1689-1703.

Hamilton., DG. and Ebersole, BA. (2001). Establishing uniform longeshore currents in a large-scale sediment transport facility. *Coastal Eng*, 42, pp.199-218, 2001.

Johnson, H.K., Brøker, I. and Zyserman, J.A (1994). Identification of some relevant processes in coastal morphological modeling. *Proceedings of the 24th International Conference on Coastal Engineering*, Kobe, Japan.

Kawaguchi,T., O. Hashimoto, T. Mizumoto and A. Kmata. (1994). Construction of offshore fishing port for prevention of coastal erosion. *Proceedings of 24th International Conference on Coastal Engineering*, 1197-1211.

Khaled Seif, A., Kuroiwa, M., Mase, H., Matsubara, Y., and Abualtayef, M. (2010). A Quasi-3D nearshore current model in wave-current coexisting field. *Annual Journal of Civil Engineering in the ocean*, JSCE,Vol.26, 297-302.

Kuroiwa, M., Matsubara, Y., Kuchiishi, T., Kato, K., Noda, H., and Son, C.B. A (2002). Morphodynamic model based on Q-3D nearshore current model and application to barred beach. *28th ICCE*, pp.3409-3421,.

Kuroiwa, M., Noda, H., Son, C.B., Kato, K., and Taniguchi, S. (2000). Numerical prediction of bottom topographical change around coastal structures using quasi-3D nearshore current model. *Proc. of the 27th ICCE*, pp.2914-2927.

Larson, M. and Kraus, N. C. NMLONG (2002). Numerical model for simulating longshore current. *Coastal and Hydraulics Laboratory Technical Report* ERDC/CHL TR-02-22. Vicksburg, MS: U.S. Army Engineer Research and Development Center.

Mase, H. (2001). Multi-directional random wave transformation model based on energy balance equation. *Coastal Eng J*., 43, No.4,

Mase, H., Yuhi, M., Amamori, H., and Takayama, T. (2004). Phase Averaging wave prediction model with breaking and diffraction effects in wave-current coexisting field. *Annual Journal of Coastal Engineering*, JSCE., 51, No.1, pp.6-10,. (In Japanese)

Sawaragi, T., Lee, J.S. and Deguchi, I. (1985). A new model for prediction of beach deformation around river mouth. *Proceedings of International Symposium on Ocean Space Utilization*, 85, 229-236.

Shibayama, T. and W. Rattanapitikon (1993). Vertical distribution of suspended sediment concentration in and out surf zone. *Coastal Eng*. in Japan, Vol.36, No.1, pp49-65.

Shimizu, T., Kumagai, T., and Watanabe, A. (1996a). Improved 3-D beach evolution model coupled with the shoreline model (3D-Shore). *Proc. of the 27th ICCE*, pp.2843-2856.

Shimizu, T., Yamda, A., and Watanabe, A. (1996b). Cross-shore distribution of alongshore sediment transport rates and its dimensionless coefficients. *Proceedings of Coastal Engineering*, JSCE, Vol.43(1), pp.571-575.

Tsuchiya, Y., Yamashita, T., and Uemoto, M (1986). A model of undertow in the surf zone. *Proceedings of the 33rd Japanese Conference on Coastal Engineering*, JSCE, pp.31-35.

Watanabe, A., Maruyama, K., Shimizu, T., and Sakakiyama, T. (1986). A numerical prediction model of three-dimensional beach deformation around a structure. *Coastal Eng*. in Japan, Vol.29, pp.179-194.

Zheng, J., Mase, H., Demirbilek, Z., and Lin, Li (2008). Implementation and evaluation of alternative wave breaking formula in a costal spectral wave model. *Ocean Eng*, 35, pp.1090-1101.